IJISEM
INTERNATIONAL JOURNAL OF INNOVATIONS IN SCIENCE ENGINEERING AND MANAGEMENT

OPEN ACCESS

Volume: 4

Issue: 3

Month: September

Year: 2025

ISSN: 2583-7117

Published: 10.09.2025

Citation:

Ashish Chourey, Piyush Kr. Verma, Pankaj Shrivastava "Thermal Comfort Analysis in Dormitory Room by Combined MVHR-Fan Coil" International Journal of Innovations in Science Engineering and Management, vol. 4, no. 3, 2025, pp. 351–363.

DOI:

10.69968/ijisem.2025v4i3351-363

Thermal Comfort Analysis in Dormitory Room by Combined MVHR-Fan Coil

Ashish Chourey[1], Piyush Kr. Verma[2], Pankaj Shrivastava[2]

[1]Research scholar, Department of Mechanical Engineering, Corporate Institute of science & technology, Bhopal, India.
[2]Asst. Prof., Department of Mechanical Engineering, Corporate Institute of Science & Technology, Bhopal.

Abstract

Low-energy-demand buildings are increasingly using "mechanical ventilation with heat recovery (MVHR)" applications to improve thermal comfort and reduce ventilation energy loss. MVHRs are often used in conjunction with an additional air heater to satisfy the need for room heating in retrofitted buildings. Therefore, it is crucial to assess how MVHR and heat emitters interact and how this affects the features of indoor airflow. In this study, the effects of a combination MVHR-fan-coil unit in the heating phase on thermal comfort parameters in a retrofitted room are investigated via "a computational fluid dynamic (CFD)" simulation. Numerical simulation results allow for the assessment of indoor thermal comfort as well as the resolution of the fan coil and MVHR interactions. Additionally, investigate the turbulent airflow characteristics in winter and summer season. The result indicate that relocate the fan coil position from left side to middle of the external wall increases the room temperature. Installing the inlet vent in ceiling shows a no changes in the room temperature. It observed that Case 2 exhibited the highest temperature inside the room at 23.3 ºC, while Case 1 and Case 3 both had a room temperature of 22.6 ºC and 22.5 ºC respectively. The average temperature across all six planes followed a similar pattern, Case 2 consistently showing higher temperatures.

Keywords; Mechanical Ventilation with Heat Recovery, Fan coil, Thermal comfort, computational fluid dynamic.

INTRODUCTION

Background

HVAC stands for air conditioning, heating, and ventilation. This system's primary concept is to provide heating and cooling to commercial as well as residential buildings [1]. In order to create safe and healthy building conditions that regulate fresh air, temperature, and humidity, HVAC is crucial in the design of medium- to large-scale industrial applications like power plants, onboard ships, office buildings like skyscrapers, and marine environments like aquariums [2], [3]. From basic air conditioning using packaged window air conditioners and single-split air conditioners for cooling, light filtration, and dehumidification to more complex air conditioning systems utilised in process plants, ships, labs, and centrally air-conditioned office buildings, air conditioning comes in a variety of forms [4], [5]. Maintaining optimal air quality, controlling humidity, and controlling temperature are all made possible by an HVAC system [6].

HVAC system requirements

The foundation of every HVAC system is four needs. HVAC system need pipe, air distribution, space, and principal equipment [7]. Examples of primary equipment include refrigeration units that disperse cooled or ventilated air into space, air circulation units that are wrapped to transport conditioned ventilation air via axial, centrifugal, or plug or plenum fans, and heating units such as steam boilers that heat buildings or spaces [8], [9]. It uses water from water chillers or coolants from a refrigeration process to cool its coils. When designing a central or local HVAC system, space requirements are crucial [10].

Ductwork that carries the heated air straight to the target area in the most direct, quiet, and efficient way possible is an important part of air distribution [11]. Air distribution includes a variety of devices, such as factor air volume terminal units, all-air induction terminal units, fan-powered terminal units, as well as air-water induction terminal units [12]. These devices control the primary air and distribute mixed air into a space, as well as contain coils in the induction air stream [13]. Stopping heat loss and saving energy may be achieved by insulating all pipes and ducts. In order to allow ducting in both the floor surface and the suspended ceiling, it is recommended that structures have sufficient ceiling spaces [14]. To reduce the quantity of return ductwork, these areas may also be utilized as “a return air plenum” [15].

"Condensate, hot water, refrigerant, steam, cooled water, and gas" are all delivered directly, silently, and affordably to and from HVAC equipment via the pipe system [16]. The delivery piping and the tube in the main plant apparatus room are the two parts that comprise piping systems. Whether or not HVAC piping is insulated depends on the current code standards [17], [18].

Indoor air quality

High concentrations of pollutants in indoor air may come from outside or ground sources, building materials and construction, furniture, appliances, and consumer goods, or from the inhabitants themselves and their activities like cooking, taking a bath, or drying clothing inside (e.g., (Markell, 2017)[19]). Certain contaminants may enter via the soil or groundwater, or from the external environment (such as PM, NO2, and CO). Building placement may have a significant impact on the amount of pollutants coming from outside sources. The (WHO, 2021) [20] offers a worldwide strategy to tackle air quality problems, taking into account regional development levels, local demographic characteristics, and time spent inside and/or outdoors. The WHO has previously released distinct criteria for outdoor and interior air quality. Target levels for a few outdoor air pollutants were set in Europe in 2000 and revised internationally in 2005. The first WHO report on the right to indoor air was released for European nations, although it made no recommendations about pollution levels. In 2010, the WHO published recommendations for a few specific indoor air pollutants, including polycyclic aromatic hydrocarbons (PAHs), benzene, CO, CH2O, and NO2. The WHO recently released global air quality standards (WHO, 2021)[20] that did not differentiate between indoor and outdoor levels of "PM2.5, PM10, ozone, NO2, sulphur dioxide, and CO". While 1-hour levels stay the same and "old" values are advised as an interim for the majority of chemicals, target yearly and 24-hour average concentrations are established at lower levels than those in 2005. In the 2021 recommendations (WHO, 2021)[20], Rn is controlled independently while CH2O and other organic pollutants identified in the 2010 document are not addressed.

RESEARCH METHODOLOGY

Governing equation

A combination of "buoyant force and momentum" causes the air to flow turbulently inside structures. The slight pressure gradient and low air velocity were predicted to make the flow incompressible. All the thermo-physical characteristics were assumed to be constant, except density, which was assumed to vary linearly with temperature. Due to the very small temperature changes inside the room, the buoyancy impact was considered using the Boussinesq approximation. The following are the mass, momentum, and energy steady-state governing equations:

$$\nabla \cdot \vec{v} = 0$$

$$\rho_0(\vec{v} \cdot \nabla)\vec{v} = -\nabla(p + \rho_0 g z) + \rho_0 g \beta (T - T_o)\nabla z + \nabla \cdot \tau_{eff}$$

$$\nabla \cdot \left(\vec{v}(\rho e + p)\right) = \nabla \cdot \left[(k + k_t)\nabla T + \tau_{eff} \cdot \vec{v}\right]$$

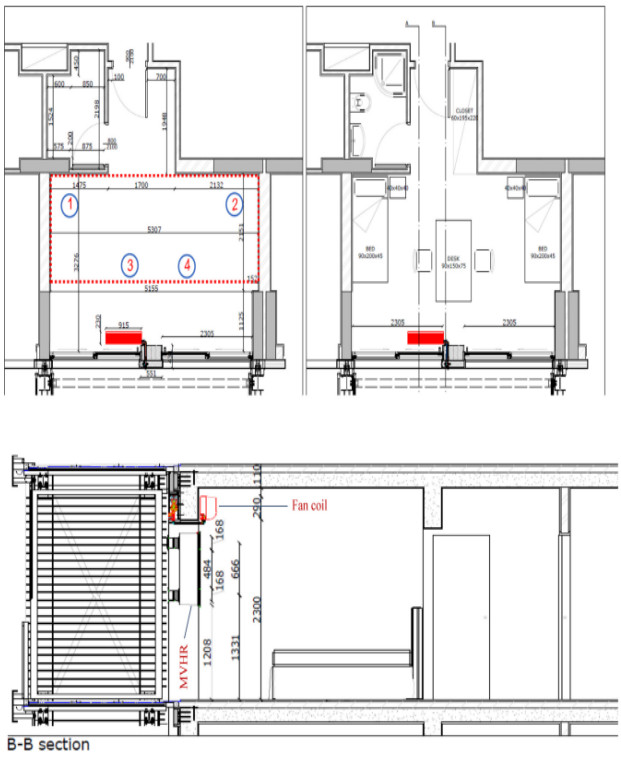

Figure 1 layout of the dorm room.

In this case, β represents the air thermal expansion coefficient, and "$\tilde{\tau}ef\ f$ is the effective stress tensor defined as $\tilde{\tau}ef\ f = \tilde{\tau} + \tilde{\tau}t$". In the Boussinesq approximation, $\tilde{\tau} = (\nabla\vec{v} + \nabla\vec{v})$ and$\tilde{\tau}t = \mu t(\nabla\vec{v} + \nabla\vec{v}T)$. In the turbulence model, "the turbulent dynamic viscosity (μt)" as well as turbulent thermal conductivity (kt) are ascertained. Moreover, the value of e, which stands for energy per mass, may be described as

$$e = h - \frac{p}{\rho} + \frac{v^2}{2}$$

Where the particular enthalpy is denoted by h.

Since "the RNG (Renormalisation Group) k-ε turbulence model" renders interior flows more accurately and with more stability, it was used in this investigation. While the RNG model is very similar to the classic κ-ε model, it has certain improvements, including an additional term in ε to improve accuracy and a differential formula to calculate effective-viscosity that allows for minimal Reynolds number effects. The RNG κ-ε model's governing equations are as follows:

$$\nabla \cdot (\rho K\vec{v}) = \nabla \cdot \left(\alpha_K \mu_{eff} \nabla K\right) + 2\mu_t E_{ij} E_{ij} - \rho\varepsilon$$

$$\nabla \cdot (\rho\varepsilon\vec{v}) = \nabla \cdot \left(\alpha_\varepsilon \mu_{eff} \nabla\varepsilon\right) + C_{1\varepsilon}^{*} \frac{\varepsilon}{K} 2\mu_t E_{ij} E_{ij} - C_{2\varepsilon}\rho \frac{\varepsilon^2}{K}$$

Eij stands for strain rate. μeff and μt have the following definitions:

$$\mu_{eff} = \mu + \mu_t; \mu_t = \rho C_\mu \frac{K^2}{\varepsilon}$$

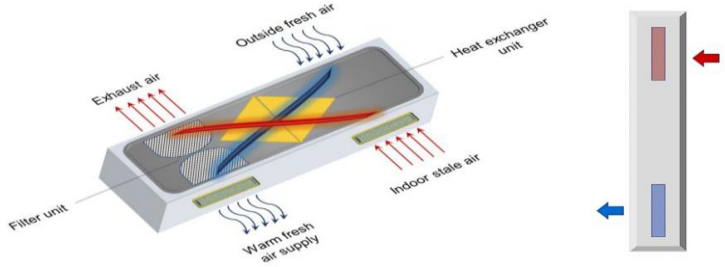

Figure 2 "The MVHR system's features (left) and lateral view (right)"

Design

An actual case study is being examined; it is a 5.31 m × 5.22 m × 2.70 m renovated dorm room at a student residence in Athens, Greece. The room domain has one outside wall with huge windows and interior walls. It is here that the fan coil and MVHR are put. The dorm room has a desk, chairs, two beds, a large closet, and two side-bed tables. Figure.1 shows the room's components' measurements and specifics. It is presumed that two students are occupying the double-room under investigation. In Figure 1, the occupied zone is shown by an outline with a red dotted line. This was done to ensure an accurate evaluation of air quality metrics inside the domain. In a horizontal configuration, 2.3 meters above ground, there is a fan coil unit that is 0.9 meters long, 0.29 meters tall, and 0.23 meters thick. The exterior façade-integrated MVHR system in use consists of a heat exchanger system, filtration unit, and input and exit ports with an identical "cross-section measure of 0.13 m × 0.02 m = 0.0026 m2". Figure 2 shows the characteristics of the used MVHR system. In this study, three computational model consider with various location of fan coil and inlet vent. In which design 1 and 2 having a fan coil in wall at left side and center respectively and design 3 having inlet vent, which is locate in the celling. In all design MVHE unit are present with no changes. Figure 3, figure 4, and figure 5 illustrate that the design 1 – fan at left, design 2 – fan at left, and design 3 – inlet vent at celling respectively with dimension use for create the model.

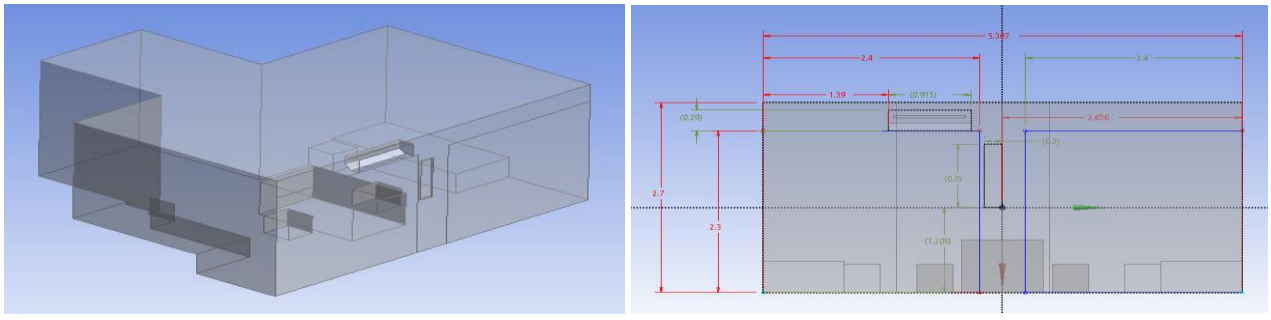

Figure 3 Computational model of design 1with essential dimension

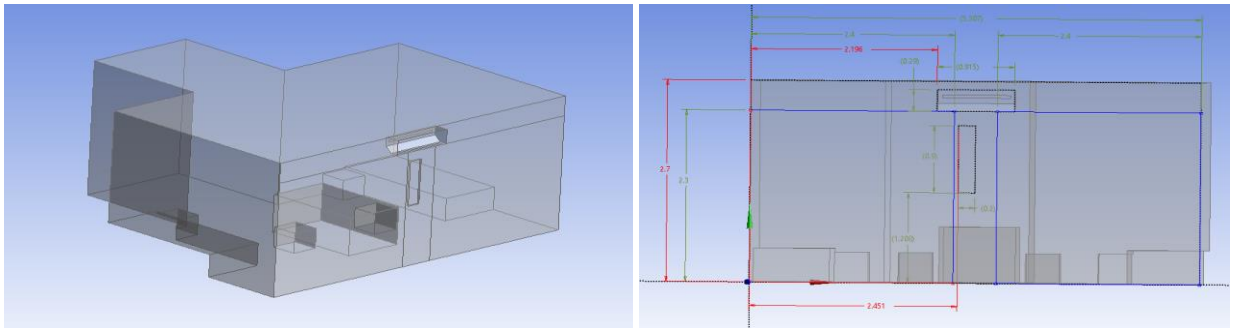

Figure 4 Computational model of design 2 – fan at center with essential dimension

Mesh generation

Tetrahedral elements were used to initially mesh the computing domain. Implement the high mesh density around the inlet and outlet. For the mesh generation ANSYS fluent select. In this process element and nodes are form for create the mesh. In all three-design element vary range of 350500 – 398300 and nodes vary range of 65600 – 74600. Figure 6 illustrate that the mesh form of computational model.

Numerical and Boundary condition

ANSYS Fluent, a CFD program, was used to construct the finite volume approach for solving "the 3D governing differential equations". This research used the "RNG (Renormalisation Group) k-ε (k-epsilon) turbulence model" because of its improved stability and accuracy while depicting interior flows. A second-order upwind approach was used to address pressure, momentum, and energy, and the coupled method was used to solve the pressure-velocity coupling. The evolution of the CFD solutions may be tracked by controlling the residual history, which displays the changes in the amount required value between two iterations. "Pressure, momentum, turbulence, and energy" components were used with relaxation factors of 0.3, 0.7, 0.8, and 1 to maximise the convergence of the solution. Table 1 reports the moist air flow and associated values of the moist air characteristics from "the fan coil and MVHR unit" intake, which were measured at reference temperature T0 = 20°C.

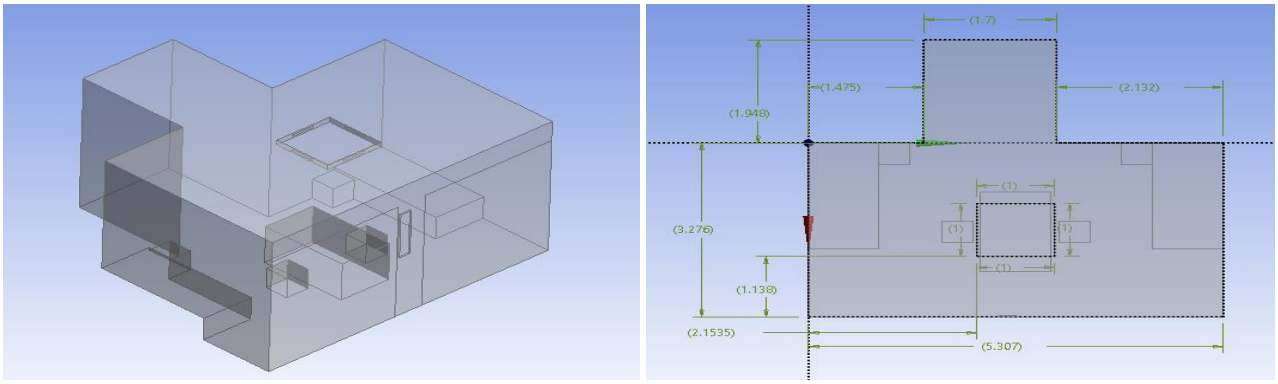

Figure 5 Computational model of design 3 with essential dimension

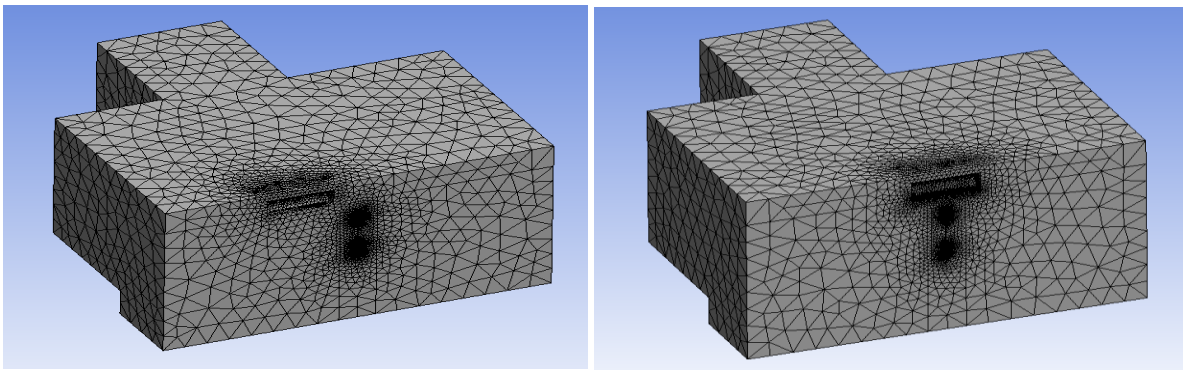

Figure 6 Mesh generation in computational domain

The outside wall was insulated during the retrofit process using cross-laminated panels that included mineral wool insulation. “Uwall = 0.33 W m−2 K−1” is the thermal transmittance of these panels. Additionally, Uwin = 0.81 W m−2 K−1 is a triple-glazed window with low-emittance coating and spectrum selective properties that is put in an exterior wall. In order to evaluate the MVHR-Fan-coil system, both summer and winter cooling and heating conditions were considered. In Athens, Greece, the average outside temperature for a normal summer day was 35 °C. In contrast to the usual winter day's lowest outside temperature of about 5 °C. Heat loss from the windows, MVHR unit, and exterior wall affects the room's thermal balance. Since a cloudy winter day is the most undesired scenario, the sun radiation was disregarded. In addition, the entry of outside air was ignored as positive pressure is often provided by the space's ventilation and air movement. The airflow leaves at a 45º angle from a 0.032 m2 cross-sectional region. Average winter temperatures are 33.8 °C, with summer highs of 21 and 19 °C, respectively. The input velocity of 3 m/s was applied to the intermediate flow rate estimate for the preliminary study. Next, the fan coil's placement is changed and replaced with an intake vent in order to assess how the fan coil's performance affects the intended parameters. All solid walls have to adhere to the non-slip requirement. In contrast to the interior walls, which were supposed to be isothermal with temperatures of 20 °C in winter and 35 °C in summer, the ceilings and floor wall surfaces were regarded as adiabatic. The exterior wall's and the windows' respective thermal transmittance values were taken into consideration: “Uwall = 0.33 W/(m2K) and Uwin = 0.81 W/(m2K)”, which are equivalent to the values previously recorded for the room during the retrofitting operation. Assumptions were made that the adiabatic state applied to the fan coil, MVHR housing, furniture, and other solid walls.

Table 1 Thermal properties of moist air

Properties	Value
Density (kg/m3)	1.153
Specific heat (J/kg K)	1019
Thermal conductivity (W/m K)	0.0253
Viscosity (kg/m s)	1.82e-5
Thermal expansivity (1/K)	0.00341

Result analysis parameter

Four locations near beds and the desk have also been chosen because they are the most likely to be occupied. The breathing zones, denoted by the numbers 1–4 (therefore p-1 to p-4 in Figure 1), are useful for making precise assessments of thermal comfort and air quality. For beds, "positions p-1 and p-2" are evaluated at 0.6 m, whereas desks, positions p-3 and p-4, are evaluated at 1.1 m, to accommodate both sitting as well as reclining postures. Six plane are consider in which see the distribution of temperature and velocity and illustrate corresponding value to compare the optimize model. Plane 1, and plane 2 lie on along the length at distance of 1.5 m and 2.5 m respectively. Plane 3, and plane 4 along the width at distance of 4.6 m and 0.5 m respectively. Plane 5, and plane 6 along the height at distance of 1.7 m, and 0.7 m respectively.

Table 2 Boundary condition for numerical simulation

Parameter	Value
Fan coil Inlet velocity	3 m/s
Inlet mean temperature	33.8 ^{o}C (Winter) 21 ^{o}C and 19 ^{o}C (Summer)
Wall thermal transmittance	0.33 $Wm^{-2}K^{-1}$
Window thermal transmittance	0.81 $Wm^{-2}K^{-1}$
External temperature	5 ^{o}C (Winter) 35 ^{o}C (Summer)
Wall surfaces of the floor and ceiling	Adiabatic

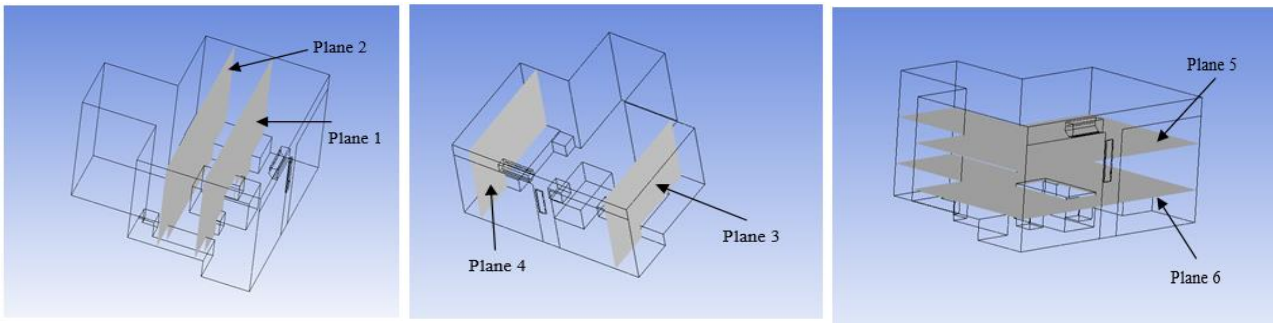

Figure 7 Plane representation

Table 3 Value of consider plane for corresponding Axis

Planes	Value
Plane 1 (XY)	1.5 m
Plane 2 (XY)	2.5 m
Plane 3 (YZ)	4.6 m
Plane 4 (YZ)	0.5 m
Plane 5 (ZX)	1.7 m
Plane 6 (ZX)	0.7 m

Numerical model validation

The numerical model was validated by comparing the outcomes of numerical simulations with those of (Jahanbin, 2022) [21]. A comparison with the numerical simulation conducted by Jahanbin (2022) [21] to ascertain the temperature within the room validates the numerical model used to estimate the turbulent airflow patterns within the room. A fan coil air velocity of 3 m/s and a temperature of 33.8 ºC are used to validate the model. Other parameter which are consider for the numerical study are describe in the boundary condition section. The comparison between both numerical results as temperature contour in plane are illustrate in the figure 8. For the validation in terms of temperature inside the room consider four point. Point 1 and 2 are at both bed and point 3 and 4 are in desk, which is in center of the room. Figure 9 illustrate the temperature value at four point in both (Jahanbin, 2022) [21] and present study and it shows good agreement with each.

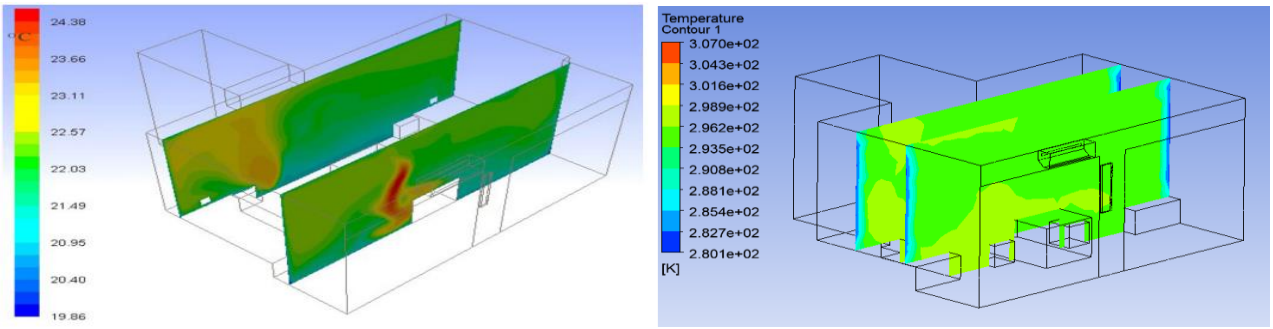

(Jahanbin, 2022)[21] Present study

Figure 8 Temperature contour comparison in plane

RESULT AND DISCUSSION

In the present study, the effectiveness of a combination MVHR-fan-coil system in providing thermal comfort in a retrofitted student residence hall is investigated numerically. Computed fluid dynamics (CFD) was created using the finite volume approach. The numerical model was verified by contrasting the outcomes of the simulations with earlier findings. In this section discussed the obtained result from the implementing the goal of this study. The result obtained in terms of distribution of temperature and velocity inside the room

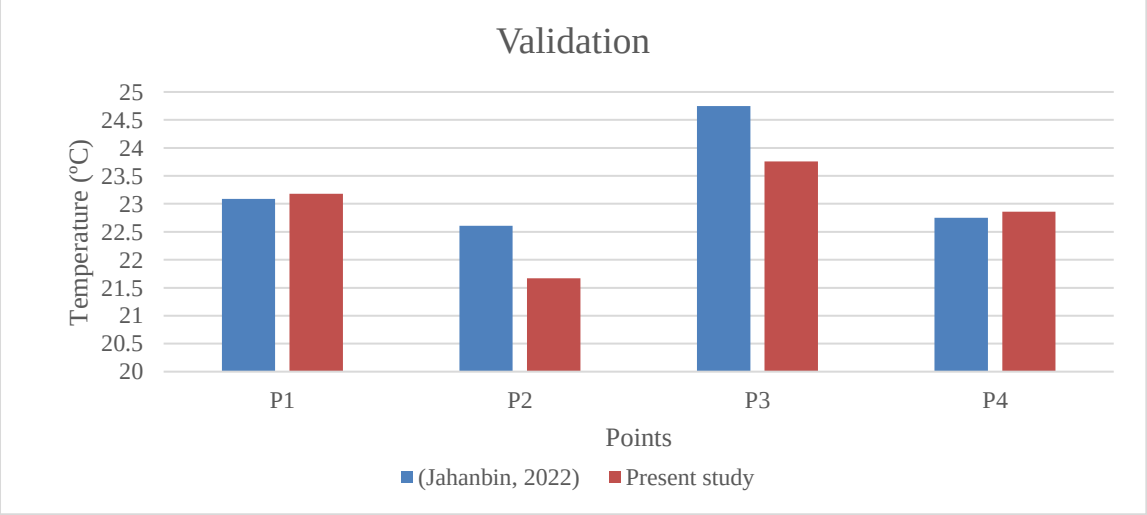

Figure 9 Temperature contour comparison in consider four point

Temperature contour

The temperature distribution within the room, derived from numerical simulations, provides crucial insights into the thermal behavior inside the enclosure, which is essential for achieving thermal comfort. Figures 10-12 show how the fan coil stream significantly affects the temperature profiles in the horizontal as well as vertical planes of the operating temperature distributions. The left half of the room has greater temperatures due to distinct flow zones with different eddies, as shown in Figure 10. The fan coil's airflow jet directly impacts this region, reaching the front wall and transferring heat over the surface to form a high-temperature zone. Except for the area next to the wall, the operating temperature is distributed in a quasi-uniform manner on the right portion of the room, with an average of around 296 K. This uniform distribution on the right side is conducive to maintaining consistent thermal comfort without significant temperature fluctuations. Figure 11 demonstrates that both sides of the room have an equal distribution of temperature, as shown in vertical planes 1-4, with an average temperature of approximately 300 K. This even distribution ensures a balanced thermal environment across the room, contributing to overall comfort. Horizontal plane 6 highlights the mixing of air, maintaining a temperature close to 300 K, which aids in creating a comfortable ambient temperature throughout the space. In the design configuration where the inlet vent is placed at the ceiling with one inlet on each side (Design 3), the temperature distribution takes on unique characteristics.

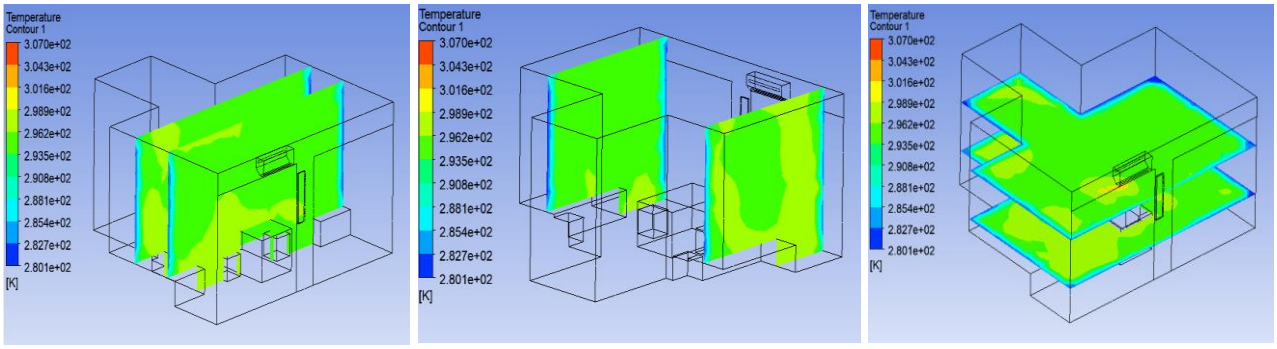

Figure 10 Temperature contour in design 1 (case 1-winter)

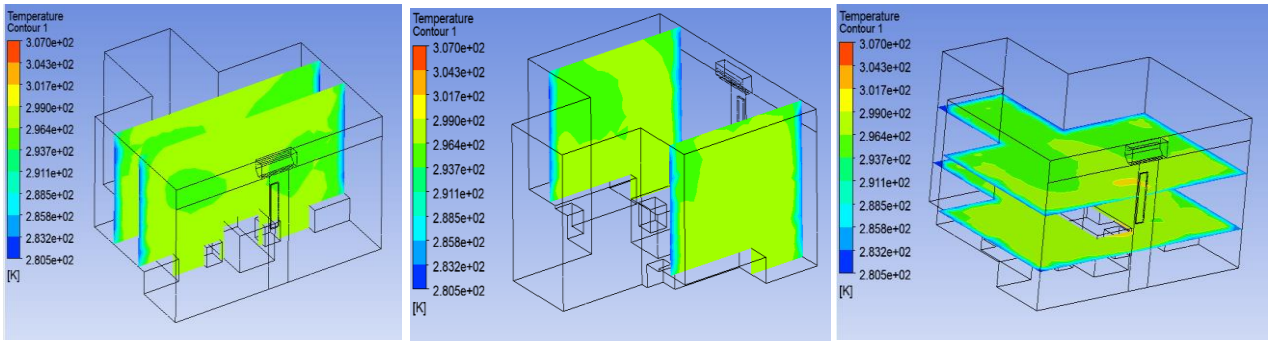

Figure 11 Temperature contour in design 2 (case 2 – winter)

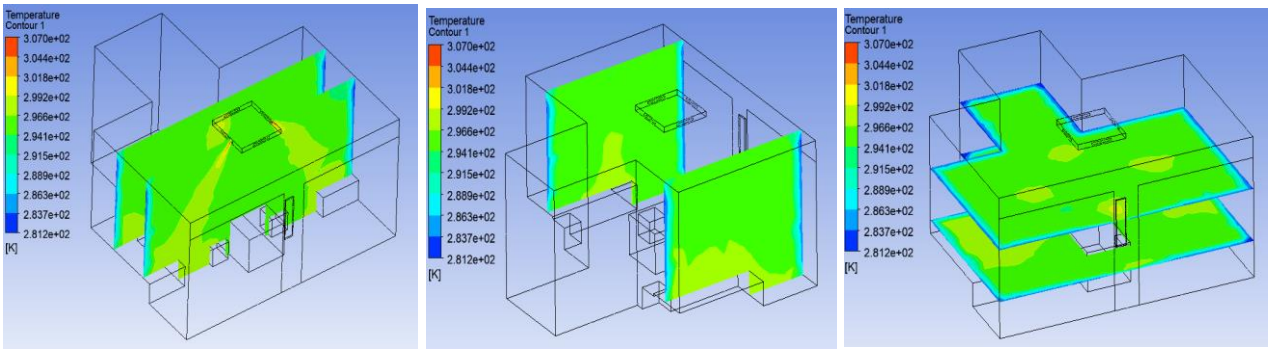

Figure 12 Temperature contour in design 3 (case 3 winter)

The vertical plane analysis indicates that the temperature distributes at an angle of 45º from the ceiling vents illustrate in figure 12. This angular distribution helps in spreading the warm air more evenly across the room, ensuring that different areas of the room are heated effectively. Horizontal plane 6 illustrates that the warm air collects at the corners where beds are placed, with temperatures around 299 K. This specific distribution suggests that strategic placement of heating vents can lead to localized areas of enhanced warmth, which can be particularly beneficial for comfort in resting areas. The simulations show that the placement and operation of the fan coil unit play a critical role in achieving thermal comfort. By ensuring that warm air is effectively distributed throughout the room, with particular attention to avoiding cold spots and maintaining a quasi-uniform temperature distribution, the overall thermal comfort can be significantly improved. For the well-being of occupants, a stable and pleasant interior atmosphere is facilitated by design configurations that encourage even heating and thoughtful airflow patterns. In order to achieve the highest level of thermal comfort in indoor environments, the comprehensive temperature distribution research ends by emphasizing how important it is to consider both vertical and horizontal planes when building and running HVAC systems.

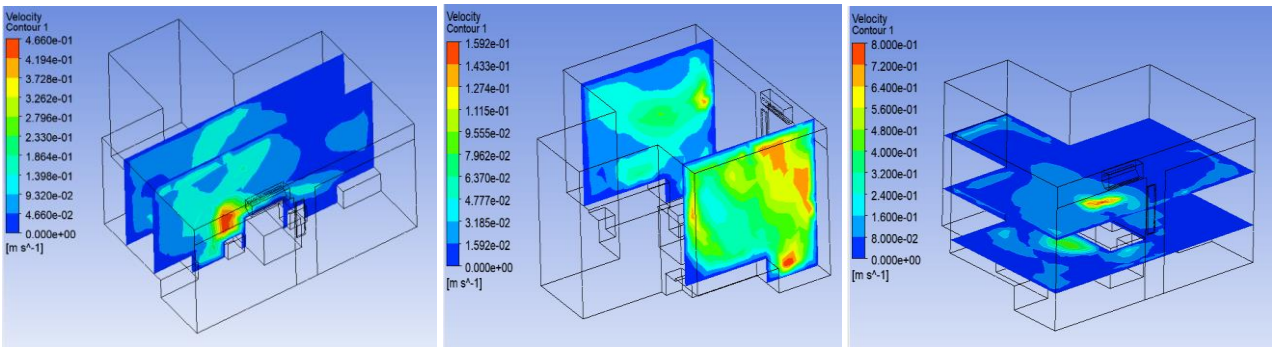

Figure 13 Velocity contours in design 1 (winter case 1)

Velocity contour

Numerical models of the room's air velocity distribution provide important insights into the workings of airflow, which are essential for attaining thermal comfort. The fan coil stream significantly affects the velocity profiles, as seen by the streamlines coloured by the magnitude of velocity at both horizontal and vertical planes 1-6 in "Figures 13 to 15". As seen in Figure 13, the velocity magnitude is larger on the left portion of the room, which has distinct flow zones with different eddies. Higher velocity zones are created in this location by the direct contact of the fan coil's airflow jet, which hits the front wall, travels along it, and turns towards the ceiling. The velocity distribution on the right side of the domain, except for the near-wall zone, is quasi-uniform, with an average velocity range of 0.06 m/s. The right-side window and "the Mechanical Ventilation with Heat Recovery (MVHR) unit" are the locations of minor vortices with smaller velocity magnitudes. The fan coil's airflow jet hits the front wall, travels along it, and then proceeds towards the ceiling, creating greater velocity zones close to the left portion of the room, as shown in vertical regional planes 1 and 2. A plume displaying a velocity value of about 0.46 m/s at plane 1 indicates that the forced convection situation is prominent ahead of the fan coil. Figure 14 demonstrates that the airflow is equally distributed on both sides of the room due to the fan coil being installed in the middle. The mean velocity in "vertical planes 1 and 2" is 0.15 m/s, while the mean velocity in planes 3 and 4 is 0.09 m/s. Small vortices form near the windows on both sides. This equal distribution ensures a balanced airflow, promoting consistent thermal comfort throughout the room.

Figure 15 indicates that in vertical planes 3 and 4, the airflow is maximized at the bottom of the room, with a magnitude of 0.15 m/s. Horizontal planes 5 and 6 display that the air reaches the front wall, further illustrating the effective distribution of airflow within the room. The detailed analysis of air velocity distribution highlights the importance of strategic placement and operation of the fan coil unit for achieving thermal comfort. The fan coil significantly influences the airflow patterns, creating zones with varying velocity magnitudes that directly affect the room's thermal environment. Ensuring a quasi-uniform distribution of airflow, especially avoiding areas of stagnant air, contributes to a stable and comfortable indoor environment. The even distribution of airflow in both horizontal and vertical planes promotes consistent thermal comfort across the room. The formation of small vortices and the presence of higher velocity zones near the walls indicate effective mixing of air, which helps maintain a comfortable temperature throughout the space. The strategic positioning of the fan coil in the

middle of the room and its operation to create forced convection conditions ensures that the air is effectively circulated, minimizing temperature variations and enhancing overall comfort. In conclusion, understanding the air velocity distribution is crucial for designing HVAC systems that achieve optimal thermal comfort. By ensuring effective and balanced airflow patterns, the indoor environment can be maintained at a comfortable and consistent temperature, enhancing occupant well-being and satisfaction.

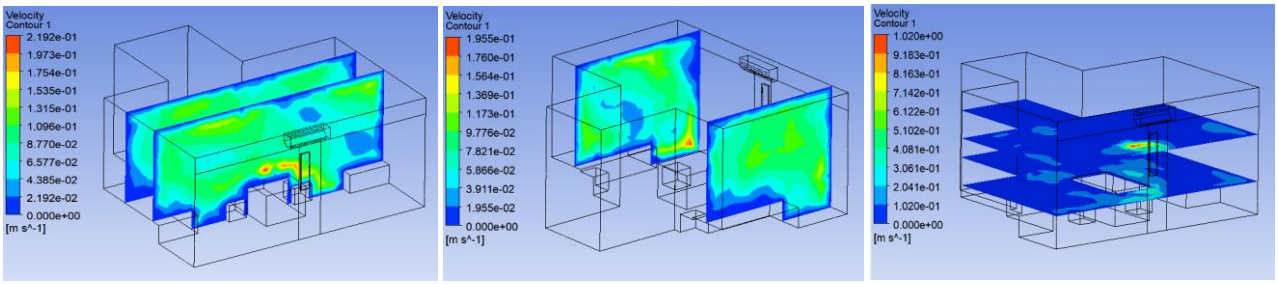

Figure 14 Velocity contours in design 2 (winter case 2)

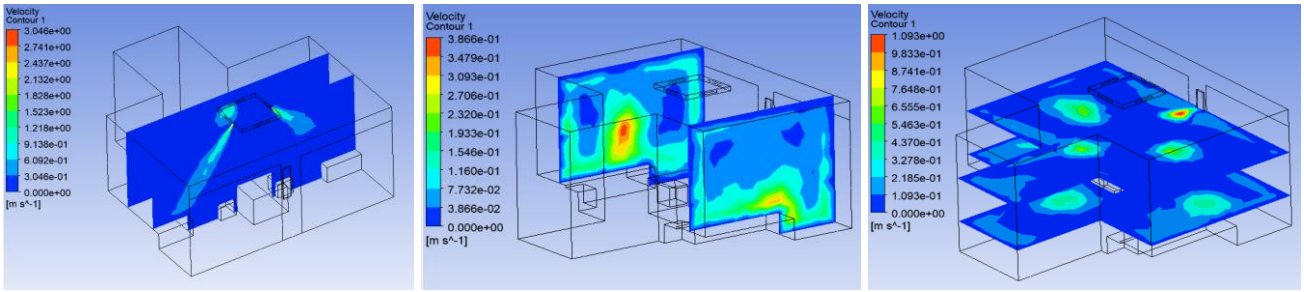

Figure 15 Velocity contours in design 3 (winter case 3)

Case 4 (summer- 19, 21ºC)

In the current scenario, the fan coil unit is installed in the middle of the external wall, a configuration referred to as Design 2. This setup remains constant, with no changes to the dimensions or placement of furniture like beds, tables, chairs, and desks. Unlike other cases that examine thermal comfort during winter with an external temperature of 5ºC, this case focuses on achieving thermal comfort inside the room during the summer season with an external temperature of 35ºC. Thermal comfort is achieved by maintaining the air velocity at 3 m/s and setting the room's temperature to either 21ºC or 19ºC.

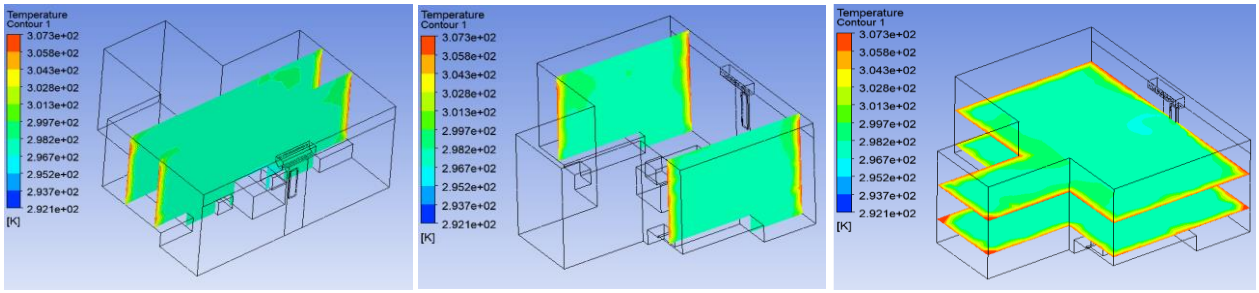

Figure 16 Temperature contour of case 4 (summer 19)

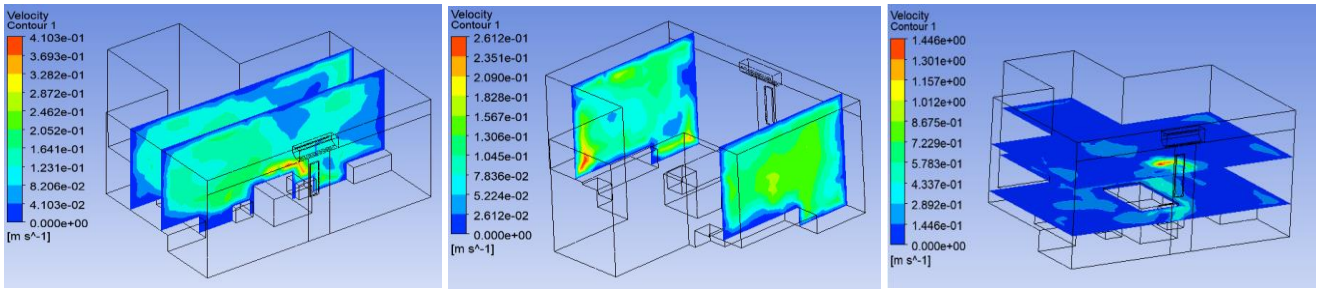

Figure 17 Velocity contour and streamlines in case 4 (summer 19)

Information on the physical behaviour of airflow within the enclosure may be gathered from numerical simulations of the temperature and air velocity distribution. Figure 16 demonstrates that both sides of the room exhibit an equal distribution of temperature, as depicted in vertical planes 1-4, with an average temperature of approximately 298 K (25ºC). This even temperature distribution ensures a balanced thermal environment across the room, contributing significantly to overall comfort. The horizontal plane 6 highlights the mixing of air, maintaining a temperature close to 298 K, which helps create a comfortable ambient temperature throughout the space. Figure 17 shows that the airflow is equally distributed on both sides of the room due to the central placement of the fan coil unit. Mean velocity is 0.16 m/s for "vertical planes 1 and 2", and 0.08 m/s for vertical planes 3 and 4. The presence of small vortices near the windows on both sides indicates effective mixing of air. This balanced airflow distribution promotes consistent thermal comfort throughout the room, ensuring that there are no significant variations in temperature or velocity that could affect occupant comfort.

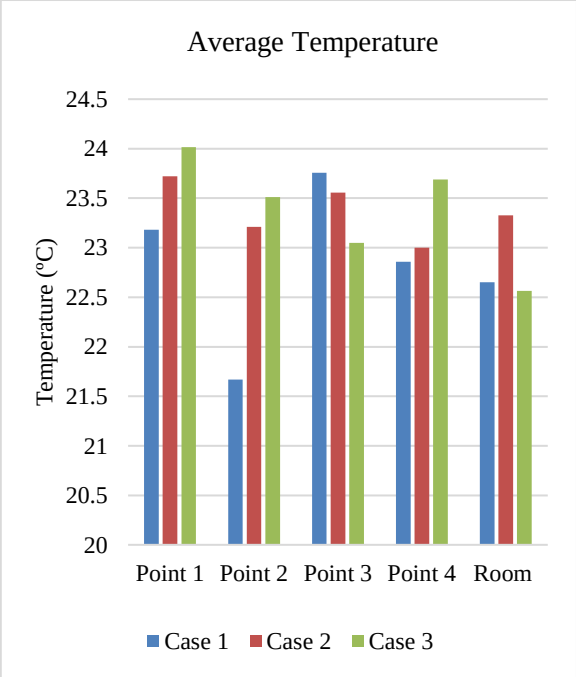

Figure 18 Average temperature in points and inside the room of case 1, 2, and 3

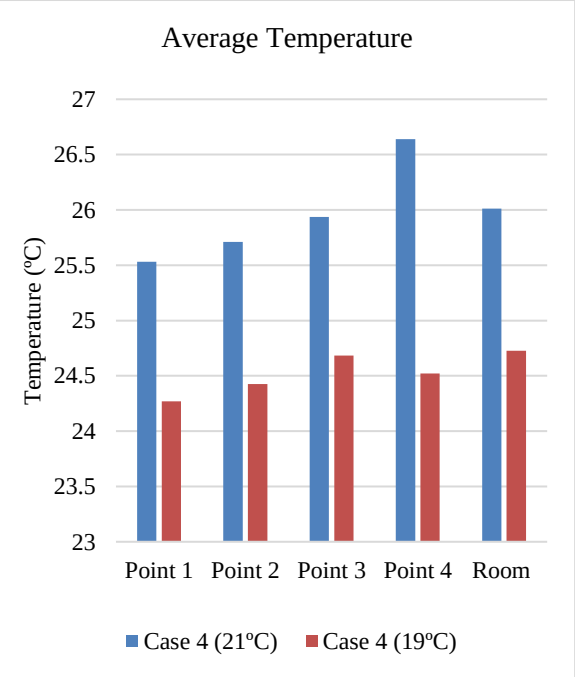

Figure 19 Average temperature in points and inside the room of case 4 with 21 and 19 ºC

In Design 2, the fan coil system is positioned in the centre of the outside wall to guarantee that the air velocity and temperature are distributed evenly throughout the space. During the summer season, with an external temperature of 35ºC, maintaining the internal air temperature at 21ºC or 19ºC and the air velocity at 3 m/s creates a stable and comfortable indoor environment. The numerical simulations illustrate that the temperature remains uniformly distributed at around 298 K, and the air velocity is balanced, promoting effective mixing and preventing hotspots or cold spots within the room. This setup effectively achieves thermal comfort, ensuring a pleasant living or working environment for occupants even in high external temperatures.

Discussion

In this study, the temperature and velocity distribution were analyzed at various points, planes, and within the entire room. Specifically, four points (Point 1-4), six vertical and horizontal planes (Plane 1-6), and the room's interior were considered. Figure 18 illustrates the average temperature for three different cases. It was observed that Case 2 exhibited the highest temperature inside the room at 23.3 ºC, while Case 1 and Case 3 both had a room temperature of 22.6 ºC and 22.5 ºC respectively. Case 1 had a very low temperature at "Points 1, 2, and 4", whereas Case 3 had the highest. On the other hand, Case 3 had the lowest temperature and Case 1 the highest at Point 3. The average temperature across all six planes followed a similar pattern, as depicted in Figure 20, with Case 2 consistently showing higher temperatures.

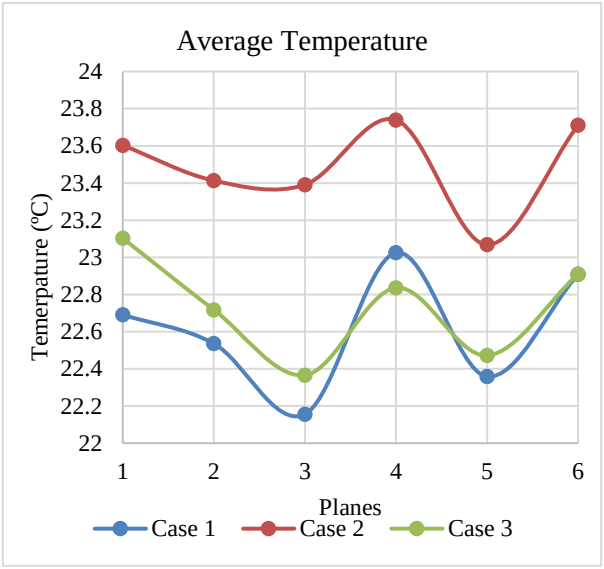

Figure 20 Average temperature in planes of case 1, 2, and 3

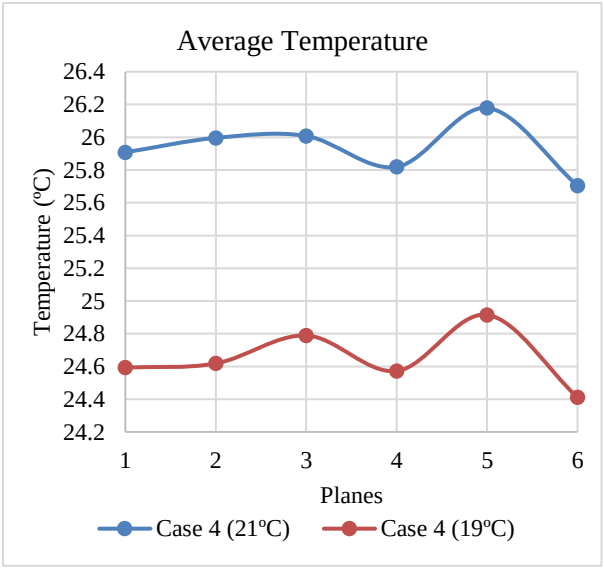

Figure 21 Average temperature in planes of case 4 with 21 and 19 ºC

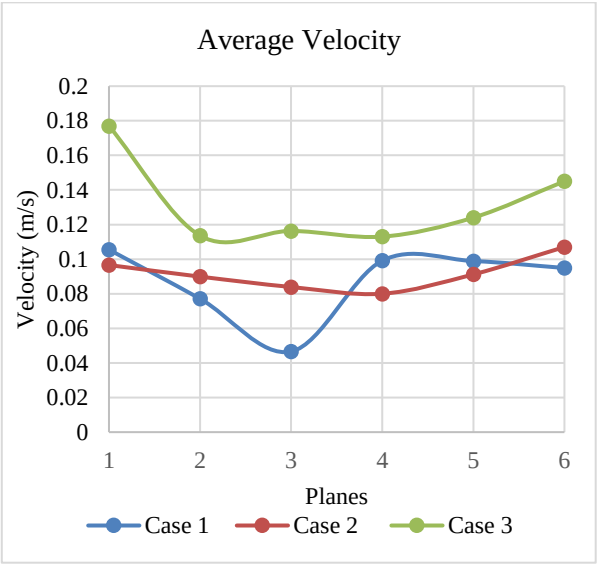

Figure 22 Average Velocity in planes of case 1, 2, and 3

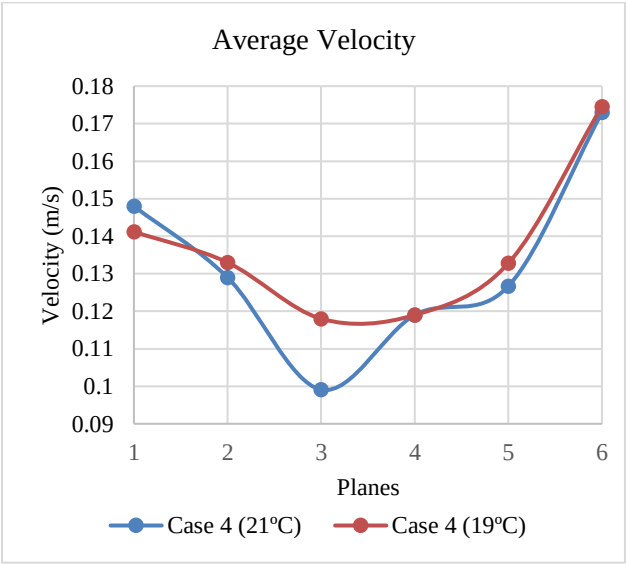

Figure 23 Average velocity in planes of case 4 with 21 and 19 ºC

Figure 19 details the average temperature at various points and within the room at inlet air temperatures of 21 ºC and 19 ºC. When the inlet temperature was 21 ºC, the inside room temperature reached 26 ºC. Conversely, with an inlet temperature of 19 ºC, the room temperature was 24.7 ºC. At an inlet temperature of 21 ºC, Point 4 had the highest temperature at 26.6 ºC, while Point 1 had the lowest at 25.5 ºC. When the inlet temperature was 19 ºC, Point 3 had the highest temperature at 24.68 ºC, and Point 1 had the lowest at 24.26 ºC. Figure 21 shows that this pattern of average temperature was consistent across all planes for both inlet temperatures, with lower inlet temperatures resulting in lower average temperatures and higher inlet temperatures leading to higher average temperatures across all planes. Finally, Figure 23 demonstrate that changes in inlet temperature did not affect the velocity patterns at the points, planes, or within the entire room. This indicates that while temperature distribution varied with inlet temperature, the velocity distribution remained constant.

CONCLUSION AND FUTURE SCOPE

Conclusion

In this work, a coupled MVHR-fan-coil system's ability to provide thermal comfort in a student residence that has undergone retrofitting is investigated numerically. The finite volume approach was used to construct "a computational fluid dynamic (CFD)" model. The findings of simulations were compared with those of earlier numerical research in order to verify the numerical code. Analyzing the turbulent air flow and operating temperature fields, as well as determining the ideal thermal comfort zones, were made possible by the results of numerical simulations. Providing thermal comfort by moving the fan coil, replacing it with an intake vent, and mounting it on the room's ceiling. Within the occupied zone, the four spots most likely to be occupied were the desk, the beds and the bathroom. Complementary simulations that included different fan coil locations and simulated winter and summer conditions were conducted in order to evaluate this impact. Ultimately, it is essential to strike a balance between recirculated and fresh airflow in envelopes with a combined HVAC system, particularly in coupled ventilation-recirculation units, in order to minimize counter flow fields, attain optimal thermal comfort, and ensure efficient fresh air circulation.

- It observed that Case 2 exhibited the highest temperature inside the room at 23.3 ºC, while Case 1 and Case 3 both had a room temperature of 22.6 ºC and 22.5 ºC respectively.
- The average temperature across all six planes followed a similar pattern, Case 2 consistently showing higher temperatures.
- An increment in the room temperature due to change the position of fan coil.
- When the inlet temperature was 21 ºC, the inside room temperature reached 26 ºC. Conversely, with an inlet temperature of 19 ºC, the room temperature was 24.7 ºC.
- At an inlet temperature of 21 ºC, Point 4 had the highest temperature at 26.6 ºC, while Point 1 had the lowest at 25.5 ºC. When the inlet temperature was 19 ºC, Point 3 had the highest temperature at 24.68 ºC, and Point 1 had the lowest at 24.26 ºC.
- When temperature distribution varied with inlet temperature, the velocity distribution remained constant.

Future scope

Future research on enhancing thermal comfort inside rooms or enclosed environments could focus on optimizing the positions of fan coil units and “Mechanical Ventilation with Heat Recovery (MVHR)” systems within the building. The placement of HVAC systems significantly influences the airflow patterns within a room, which in turn affects thermal comfort. By strategically positioning fan coil units and MVHR systems, it is possible to achieve more uniform temperature distribution and improved air circulation. This could involve experimenting with various configurations to determine the most effective arrangements for different room layouts and sizes. Additionally, understanding the interaction between the airflow patterns and inlet flow rates at different HVAC positions could lead to the development of more efficient systems that not only enhance thermal comfort but also improve energy efficiency. Advanced computational fluid dynamics (CFD) simulations and real-world experiments could be employed to identify optimal positions and configurations, ensuring that HVAC systems contribute to a more comfortable and energy-efficient indoor environment.

REFERENCES

[1] Y. Geng, W. Ji, B. Lin, and Y. Zhu, “The impact of thermal environment on occupant IEQ perception and productivity,” *Build. Environ.*, vol. 121, pp. 158–167, 2017, doi: 10.1016/j.buildenv.2017.05.022.

[2] S. Seyam, “Types of HVAC Systems,” *HVAC Syst.*, 2018, doi: 10.5772/intechopen.78942.

[3] C. Marino, A. Nucara, and M. Pietrafesa, “Thermal comfort in indoor environment: Effect of the solar radiation on the radiant temperature asymmetry,” *Sol. Energy*, vol. 144, pp. 295–309, 2017, doi: 10.1016/j.solener.2017.01.014.

[4] X. Su, Y. Yuan, Z. Wang, W. Liu, L. Lan, and Z. Lian, “Human thermal comfort in non-uniform thermal environments: A review,” *Energy Built Environ.*, vol. 5, no. 6, pp. 853–862, 2024, doi: 10.1016/j.enbenv.2023.06.012.

[5] M. W. Ahmad, M. Mourshed, B. Yuce, and Y. Rezgui, “Computational intelligence techniques for HVAC systems: A review,” *Build. Simul.*, vol. 9, no. 4, pp. 359–398, 2016, doi: 10.1007/s12273-016-0285-4.

[6] E. Zender – Świercz, “Improvement of indoor air quality by way of using decentralised ventilation,”

J. Build. Eng., vol. 32, p. 101663, 2020, doi: 10.1016/j.jobe.2020.101663.

[7] A. H. Poshtiri and S. M. Mohabbati, "Performance analysis of wind catcher integrated with shower cooling system to meet thermal comfort conditions in buildings," *J. Clean. Prod.*, vol. 148, pp. 452–466, 2017, doi: 10.1016/j.jclepro.2017.01.160.

[8] C. Buratti and D. Palladino, "Mean age of air in natural ventilated buildings: Experimental evaluation and CO2 prediction by artificial neural networks," *Appl. Sci.*, vol. 10, no. 5, pp. 1–22, 2020, doi: 10.3390/app10051730.

[9] D. Lai and Q. Chen, "A two-dimensional model for calculating heat transfer in the human body in a transient and non-uniform thermal environment," *Energy Build.*, vol. 118, pp. 114–122, 2016, doi: 10.1016/j.enbuild.2016.02.051.

[10] Z. Chen, J. Xin, and P. Liu, "Air quality and thermal comfort analysis of kitchen environment with CFD simulation and experimental calibration," *Build. Environ.*, vol. 172, no. December 2019, p. 106691, 2020, doi: 10.1016/j.buildenv.2020.106691.

[11] A. Awwad, M. H. Mohamed, and M. Fatouh, "Optimal design of a louver face ceiling diffuser using CFD to improve occupant's thermal comfort," *J. Build. Eng.*, vol. 11, pp. 134–157, 2017, doi: 10.1016/j.jobe.2017.04.009.

[12] F. Mancini, F. Nardecchia, D. Groppi, F. Ruperto, and C. Romeo, "Indoor environmental quality analysis for optimizing energy consumptions varying air ventilation rates," *Sustain.*, vol. 12, no. 2, 2020, doi: 10.3390/su12020482.

[13] G. Semprini, A. Jahanbin, B. Pulvirenti, and P. Guidorzi, "Evaluation of thermal comfort inside an office equipped with a fan coil HVAC system: A CFD approach," *Futur. Cities Environ.*, vol. 5, no. 1, pp. 1–10, 2019, doi: 10.5334/fce.78.

[14] J. Fernandez-Aguera, M. Á. Campano, S. Dom, I. Acosta, and J. Jos, "COants ' S2 Concentration and Occupymptoms in Mediterranean Climate," *Buildings*, 2019.

[15] X. Ye, Y. Kang, F. Yang, and K. Zhong, "Comparison study of contaminant distribution and indoor air quality in large-height spaces between impinging jet and mixing ventilation systems in heating mode," *Build. Environ.*, vol. 160, no. February, p. 106159, 2019, doi: 10.1016/j.buildenv.2019.106159.

[16] S. Torresin, G. Pernigotto, F. Cappelletti, and A. Gasparella, "Combined effects of environmental factors on human perception and objective performance: A review of experimental laboratory works," *Indoor Air*, vol. 28, no. 4, pp. 525–538, 2018, doi: 10.1111/ina.12457.

[17] H. Amai, S. Liu, and A. Novoselac, "Experimental study on air change effectiveness: Improving air distribution with all-air heating systems," *Build. Environ.*, vol. 125, pp. 515–527, 2017, doi: 10.1016/j.buildenv.2017.09.017.

[18] I. Technology, "Thermal comfort and indoor air quality," *Green Energy Technol.*, vol. 84, no. 3, pp. 1–13, 2012, doi: 10.1007/978-1-4471-2336-1_1.

[19] L. C. Markell, "Indoor air quality," *ASHRAE J.*, vol. 59, no. 6, pp. 12–13, 2017.

[20] WHO, "WHO global air quality guidelines," *Part. matter (PM2.5 PM10), ozone, nitrogen dioxide, sulfur dioxide carbon monoxide.*, pp. 1–360, 2021.

[21] A. Jahanbin, "Efficacy of coupling heat recovery ventilation and fan coil systems in improving the indoor air quality and thermal comfort condition," *Energy Built Environ.*, vol. 3, no. 4, pp. 478–495, 2022, doi: 10.1016/j.enbenv.2021.05.005.